Exact task execution in highly under-actuated soft limbs: an operational space based approach

Cosimo Della Santina, Lucia Pallottino, Daniela Rus, Antonio Bicchi

***Abstract*—Recently, the development of soft robots is imposing a change of prospective in several aspects of design and control, moving the robotic field closer to the natural world. Soft robots, like many animals, are often built of continuously deformable elements, and consequently are characterized by a highly under-actuated input space. In this paper we prove that given a generic nonlinear task to be accomplished by a soft robot - as e.g. the positioning of its end effector in space - a linear actuation space with the size of the task itself is already sufficient to achieve the goal. We then introduce the dynamically consistent projector into synergistic space, which can be used to convert controllers designed in operational space, to work in the under-actuated case. This enables a direct translation of control strategies from classic to soft robotics. Leveraging on this result, we present the first dynamic feedback controller for trunk-like soft robots taking in account non constant deformations of the soft body. We present simulations showing that using this controller it is possible to track a prescribed dynamic evolution of the robot's tip with zero error at steady state, both in planar and 3D case with gravity.**

***Index Terms*—Modeling, Control, and Learning for Soft Robots; Redundant Robots; Natural Machine Motion; Soft Robot Applications; Motion Control.**

I. Introduction

BOTH vertebrate and invertebrate animals are able to manage their body with high precision, despite the high under-actuation of neuro-muscle-skeletal system. On the opposite, controllers of classic rigid robots often rely on a fully actuated input space which is exploited to force the whole dynamics to behave according to a prescribed behavior. Soft robots gained considerable attention in the last few years, thanks to their ability to solve in new and more effective ways problems often unsolved by classic rigid bodied robots [1], [2]. Nonetheless, while considerable efforts have been dedicated to building soft bodies, relatively few works have dealt the problem of developing effective brains, i.e. controllers [3]. A main reason behind this shortage of results can be regarded as being the lack of dynamic models, preventing the application of model-based techniques. In recent years, this gap has been filled by the introduction of several kinematic [4] and dynamic models [5]–[8]. However, a main limitation in translating control results from classic robotics to the soft world still persists; standard control strategies typically assume a fully actuated space [9], while continuum soft robots are inherently under-actuated[1]. In [10] we faced this issue by proposing a model approximation, based on the space discretization of the robot in a set of constant curvature segments, in number equal to the actuators. This effectively produces a fully actuated model, that we used to design controllers with encouraging experimental results. However, this approach has obvious limitations in managing deformations with non constant curvature, as the ones produced by external or inertial forces. So finding a general way of dealing with under-actuation in soft bodied robots can be regarded as one of the main challenges in soft robot control.

Furthermore, under-actuation appears not only as an inevitable practical requirement, but also as a goal to be actively pursued. In rigid robots, a fully actuated input space is ideal since it can be exploited to wash out the physical properties of the system, imposing a prescribed behavior. In contrast, soft robots embody an high degree of intelligence directly in their bodies [11], and over-constraining them through control can bring to a removal of that intelligence [12]. Likewise, in the animal kingdom under-actuation is as pervasive as softness. The animal muscles are organized in low dimensional patterns of activation, called muscle synergies [13]. Plenty of examples exist of soft bodied animals controlling their bodies by using reduced input spaces (e.g. octopuses [14], elephants [15]).

This work faces the problem of designing controllers for highly under actuated soft robots, in the case of serial or tree shaped soft limbs (see e.g. Fig. 1). First, we show that the minimum number of linear patterns of actuation, needed to execute a generic nonlinear task, is equal to the dimension of the task itself. For example, three actuation sources acting along a soft limb can move the robot's tip in space, regardless the robot length and shape. Despite the apparent simplicity of the result, this property is not at all obvious for at least two reasons. First, the task to be accomplished has in general a non-linear relationship with the robot's configuration, while actuators act here linearly on

Manuscript received: October, 15, 2018; Revised January 11, 2019; Accepted March 8, 2019. This paper was recommended for publication by Editor Kyu-Jin Cho upon evaluation of Reviewers' comments. This work was supported by the National Science Foundation (grant NSF 1830901 and NSF 1226883), and by the European Union's Horizon 2020 research and innovation programme under Grant Agreement 645599 (Soma). The work was partially supported by the Italian Ministry of Education and Research (MIUR) in the framework of the CrossLab project (Departments of Excellence). We are grateful for this support.

C. Della Santina, L. Pallottino, and A. Bicchi are with Centro E. Piaggio, and the Dept. of Information Engineering, University of Pisa, Italy, cosimodellasantina@gmail.com, lucia.pallottino@unipi.it

A. Bicchi is with "Soft Robotics for Human Cooperation and Rehabilitation" Lab, Istituto Italiano di Tecnologia, Genoa, Italy, antonio.bicchi@iit.it

D. Rus and C. Della Santina are with the Computer Science and Artificial Intelligence Laboratory, Massachusetts Institute of Technology, 32 Vassar St., Cambridge, MA 02139, USA, rus@csail.mit.edu

Digital Object Identifier (DOI): see top of this page.

[1]The virtually infinite number of degrees of freedom can not be matched by a same number of actuators.

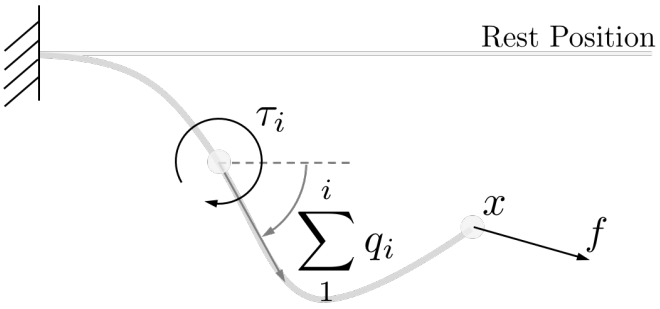

Figure 1. Schematic representation of a planar serial soft arm, with main quantities highlighted. The configuration is described by $q \in \mathbb{R}^n$ - with q_i as its $i-$th element - which here collects the local changes of orientation w.r.t. the horizontal. A torque $\tau \in \mathbb{R}^n$ is applied along the limb. For the sake of clarity only the $i-$th element τ_i is reported in figure. In this example, the task variables $x \in \mathbb{R}^2$ are the end effector position. The theory proposed in this paper enables the design of controllers which can implement a desired behavior in task space, even with an input space of very reduced dimensionality - two in this example.

the system. Second, the behavior of the robot in task space is strongly affected by couplings with the whole soft body. Thus, the reduced input space has to manage effects which are inherently high dimensional.

We then introduce the *dynamically consistent projector in synergistic space*, which allows to convert a large class of controllers designed for fully actuated system, to the reduced dimensional input case. The new controller maintains all the convergence characteristics in terms of task accomplishment of the previous one. Finally, we propose an extension to the soft-bodied case of the classic operational space controller proposed in [16], and we use it to control the position of the tip of a serial soft robot. We validate the proposed results in simulation on a 2D arm placed on a planar surface, and on a 3D soft limb moving in space.

To summarize, this paper contributes with

- A theoretical assessment of possibilities and limits in nonlinear dynamic task accomplishment with soft robots;
- A constructive way of translating existing dynamic controllers to work in the soft robot case;
- The first model based dynamic controller for soft robots tacking in account not constant deformations of the soft body;
- Extensive simulations assessing the controller effectiveness in nominal conditions.

II. Dynamics, Task Space and Synergies

Soft robots have continuously deformable bodies, thus their dynamics is naturally formulated as an infinite dimensional system [17]. However, in recent years several works [5]–[8] have been proving that more standard ordinary differential equations can be used to describe robot behavior at any level of accuracy. Leveraging on these results, we consider in this work a generic soft robot as described by the following set of ordinary differential equations

$$B(q)\ddot{q} + C(q,\dot{q})\dot{q} + G(q) + Kq + D\dot{q} = \tau \ , \qquad (1)$$

where $q \in \mathbb{R}^n$ is the configuration space, with its time derivatives $\dot{q}, \ddot{q} \in \mathbb{R}^n$. $B(q) \in \mathbb{R}^{n\times n}$ is the inertia matrix, $C(q,\dot{q})\dot{q} \in \mathbb{R}^n$ collects centrifugal and Coriolis effects, and $G(q) \in \mathbb{R}^n$ takes into account the effect of gravity. The impedance of the robot is consider for simplicity linear. However, most of the results proposed are easily generalizable to the nonlinear case. $K \in \mathbb{R}^{n\times n}$ is the robot's stiffness, and $D \in \mathbb{R}^{n\times n}$ is the damping. Both matrices are symmetric and positive defined. A set of torques $\tau \in \mathbb{R}^n$ are applied to the robot. A full and exact knowledge of the model will be assumed in the following.

Note that no explicit constraints are imposed in (1). Among the other things, this implies that we are taking in consideration trunk-like soft manipulators (i.e. serial), or soft systems with tree topology (e.g. a soft upper body with not interacting limbs). Future work will be devoted to extending our results to closed chains, and non holonomic soft robots.

A common way of describing a task to be accomplished by the robot is by introducing the following output function

$$\begin{aligned} x &= h(q) \ , \quad h(\cdot) : \mathbb{R}^n \to \mathbb{R}^m \\ \dot{x} &= J(q)\dot{q} \ , \quad J(q) \triangleq \frac{\partial h}{\partial q} \ . \end{aligned} \qquad (2)$$

We call $x \in \mathbb{R}^n$ configuration in task or operational space. The prescribed behavior is defined through a desired (possibly time variant) task configuration x_{d}. The goal of the controller is to generate an actuation pattern τ, such that x eventually converges to x_{d}. A common choice for $h(q)$ is the direct kinematics of the robot's tip [18], albeit its applicability is much broader [19]. The only properties that we ask $h(q)$ to have are i) to be continuously differentiable ii) to have a Jacobian $J(q)$ with full rank almost everywhere. We will refer to $m = \mathrm{Rank}\{J(q)\}$ as dimension of the task. Given the discussed high dimensionality of the state space, in the soft robot case

$$m << n \ . \qquad (3)$$

As an example, Fig. 1 shows a planar soft robot with main quantities underlined.

In his seminal work [16], Khatib proposed to express the dynamics of the task directly in terms of x. For a system in the form of (1), the following operational space dynamics results

$$\begin{aligned} &\Lambda_x(q)\,\ddot{x} + \eta(q,\dot{q}) \\ &\qquad + J_B^{+\mathrm{T}}(q)\,(G(q) + Kq + D\dot{q}) = J_B^{+\mathrm{T}}(q)\,\tau \ . \end{aligned} \qquad (4)$$

Where $J_B^+ \in \mathbb{R}^{n\times m}$ is the dynamically consistent pseudo-inverse

$$J_B^+(q) = B^{-1}(q)\,J^{\mathrm{T}}(q)\,\left(J(q)\,B^{-1}(q)\,J^{\mathrm{T}}(q)\right)^{-1} \ , \qquad (5)$$

$\Lambda(q) \in \mathbb{R}^{m\times m}$ is the inertia matrix of the task space, and $\eta(q,\dot{q}) \in \mathbb{R}^m$ collects the Coriolis and centrifugal terms. We refer to [16] for the closed forms of these matrices in terms of elements in (1).

Leveraging on (4), control strategies can be designed such that $x \to x_d$. The development of such a controller is a classic result in the rigid case, and articulated soft robot case [20]. In all these previous works, a fully actuated model is

considered, and the control action in torque space is produced by taking

$$\tau = J^{\mathrm{T}}(q)\, f\,, \tag{6}$$

where $f \in \mathbb{R}^m$ is a generic wrench applied in task space (see Fig. 1). Indeed, plugging (6) into (4) yields the following fully actuated dynamics in task space

$$\Lambda_x(q)\,\ddot{x} + \eta(q,\dot{q}) + J_B^{+\mathrm{T}}(q)\,(Kq + G(q) + D\dot{q}) = f\,, \tag{7}$$

that can then be used to design control strategies directly in task space.

In the general case, (6) spans all the input space $\mathbb{R}^n$, when varying f in $\mathbb{R}^m$ and q in $\mathbb{R}^n$. However, while mathematically feasible, requiring each torque to be exerted independently is overly stringent, and not practically implementable, since it would require a too dense distribution of actuators. So, as for synergies in animals, we consider

$$\tau \in \mathrm{Span}\{S\}\,, \quad S \in \mathbb{R}^{n\times k} \text{ s.t. } \mathrm{Rank}\{S\} = k\,. \tag{8}$$

In analogy to the natural example, we refer to $\mathrm{Span}\{S\}$ as *space of synergistic activations*, of which the columns of S are a base. As in natural synergies each column of S describes a coordinate patter of activation in the soft robot's input space, i.e. a direction in which the actuation is exerted. We will call S *synergies matrix*. The exact knowledge of S is considered available in the rest of the paper. These directions of actuations can be designed and implemented through a variety of technologies, as electro-active polymers [21], tendons [22], and soft fluid elastomer [23].

III. Synergistic Control

The following theorem deals with the problem of understanding which is the minimum k, for which the synergy matrix $S \in \mathrm{R}^{n\times k}$ defines an input space sufficiently rich to include all control actions needed to freely act on the task space. The key idea of the theorem is accepting to produce a residual torque τ_{r}, that can compensate for the components of $J^{\mathrm{T}}(q)f$ outside of $\mathrm{Span}\{S\}$, while remaining dynamically consistent with the task. The impossibility of fully decoupling nullspace from operational space when some degrees of freedom are not actuated was first recognized in [24].

Theorem 1. *Given an under-actuation pattern described by the matrix $S \in \mathbb{R}^{n\times m}$, the control action*

$$\tau = J^{\mathrm{T}}(q)f + \tau_{\mathrm{r}}(q,f;S) \tag{9}$$

with

$$\tau_{\mathrm{r}}(q,f;S) = (S(JB^{-1}S)^{-1}JB^{-1} - I)J^{\mathrm{T}}f \tag{10}$$

is such that

$$\tau \in \mathrm{Span}\{S\} \quad \forall q, f, S \tag{11}$$

and it generates the fully actuated operational space dynamics (7) *if*

$$\mathrm{Rank}\{JB^{-1}S\} = m\,. \tag{12}$$

Proof. Condition (11) can be reformulated as

$$\exists \sigma \in \mathbb{R}^m \quad \text{s.t.} \quad S\sigma = J^{\mathrm{T}}(q)f + \tau_{\mathrm{r}}(q,f;S)\,. \tag{13}$$

Having a fully actuated operational dynamics in the form of (7) is instead equivalent to asking that (see (4))

$$f = J_B^{+\mathrm{T}}\tau = J_B^{+\mathrm{T}}J^{\mathrm{T}}(q)f + J_B^{+\mathrm{T}}\tau_{\mathrm{r}}\,. \tag{14}$$

Considering that $J_B^{+\mathrm{T}}J^{\mathrm{T}}(q) = I$, this can be reformulated as

$$J_B^{+\mathrm{T}}\tau_{\mathrm{r}} = 0 \Leftrightarrow J(q)B^{-1}(q)\tau_{\mathrm{r}} = 0\,, \tag{15}$$

which is implied by the invertibility of $\left(J(q)\,B^{-1}(q)\,J^{\mathrm{T}}(q)\right)^{-1}$. Note that $J(q)B^{-1}(q)\tau_{\mathrm{r}} = 0$ is the well known condition of dynamic consistency [20].

Eq.s (13) and (15) can be reformulated in matrix form as

$$\begin{bmatrix} -I & S \\ J(q)B^{-1}(q) & 0 \end{bmatrix}\begin{bmatrix} \tau_{\mathrm{r}} \\ \sigma \end{bmatrix} = \begin{bmatrix} J^{\mathrm{T}}(q)f \\ 0 \end{bmatrix}\,. \tag{16}$$

This is a linear problem, with $n+m$ unkowns and $n+m$ equations. Furthermore, the block matrix in (16) is full rank if $JB^{-1}S$ is full rank, which holds by hypothesis. Thus, through block-inversion [25] we can conclude the proof by evaluating $\tau_{\mathrm{r}}(q,f;S)$ and $\sigma(q,f;S)$

$$\begin{cases} \tau_{\mathrm{r}}(q,f;S) &= (S(JB^{-1}S)^{-1}JB^{-1} - I)J^{\mathrm{T}}f \\ \sigma(q,f;S) &= (JB^{-1}S)^{-1}JB^{-1}J^{T}f\,. \end{cases} \tag{17}$$

□

Remark 1. *Note that*

$$\tau = J^{\mathrm{T}}f + \tau_{\mathrm{r}}(q,f;S) = S(JB^{-1}S)^{-1}JB^{-1}J^{T}f\,. \tag{18}$$

Thus the matrix

$$P_{S,B}(q) \doteq \left(J(q)B^{-1}(q)S(q)\right)^{-1}J(q)B^{-1}(q) \tag{19}$$

assumes the role of a dynamically consistent projector into the synergistic space $\mathrm{Span}\{S\}$. *Indeed,* (9) *can be equivalently expressed as*

$$\begin{cases} \tau &= S\sigma \\ \sigma &= P_{S,B}(q)J^{\mathrm{T}}(q)f\,. \end{cases} \tag{20}$$

Here a force $f \in \mathbb{R}^m$ generated by a generic controller designed in operational space (4) is first projected in the fully actuated input space $\mathbb{R}^n$ by pre-multiplication for $J^{\mathrm{T}}(q)$. $J^{\mathrm{T}}(q)f$ it is then transformed in a low dimensional input $\sigma \in \mathbb{R}^m$ by $P_{S,B}(q)$. σ is then mapped to the torques $\tau \in \mathrm{Span}\{S\} \subset \mathbb{R}^n$, through the under-actuation model - i.e. pre-multiplication for S. In this way controllers designed for classic fully actuated robots (Fig. 2(a)) can be directly adapted to the soft case (Fig. 2(b)). We will provide in next section an example of application of this control design technique.

Remark 2. *The necessary and sufficient condition* (12) *is equivalent to asking that any f produces at least some acceleration in the direction of S. Indeed*

$$\begin{aligned} &\mathrm{Rank}\{JB^{-1}S\} = m \\ \Leftrightarrow &\mathrm{Rank}\{S^{\mathrm{T}}B^{-1}J^{\mathrm{T}}\} = m \\ \Leftrightarrow &S^{\mathrm{T}}(B^{-1}J^{\mathrm{T}}f) \neq 0 \quad \forall f \in \mathbb{R}^m \setminus \{0\} \end{aligned} \tag{21}$$

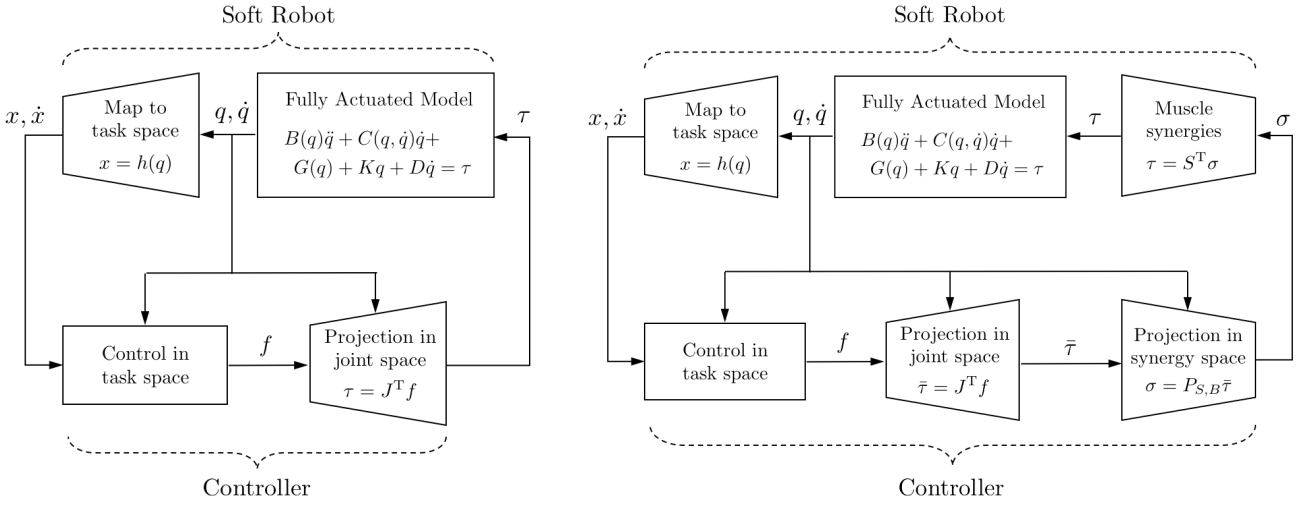

(a) Fully actuated (b) Under actuated

Figure 2. If the soft robot is imagined to be fully actuated (not feasible in practice) then a vast literature can be used to design controllers. Panel (a) shows the block scheme in the case of a controller designed in operational space. The controller is made of two components; a main part producing the control action in task space f - called *Control in task space* in figure - and a projection, mapping f into τ. However, in the practice soft robots are highly under actuated. We model this by constraining τ to span a subspace of $\mathbb{R}^n$, which can be as small as the task space. This is implemented by the *Muscle synergies* block, in panel (b). The here proposed dynamically consistent projector in the synergies space $P_{S,B}$ extends controllers designed in the previous case, to the more practically reasonable under actuated case. Trapezoids are used in the figure to visually represent the reduction or increment of dimensionality.

where we exploited the symmetry of B^{-1}. Note that $B^{-1}J^{\mathrm{T}}f$ is the acceleration induced at the joint level by a force f applied in the operational space.

Note that, while per se generically applicable, the result presented in this section requires the robot to be able to absorb a torque τ_{r} without being destabilized. This is typically not true for a rigid robot. Instead soft robots present a self stabilizing property already recognized by previous works, e.g. [10], [26], [27]. This is confirmed by the result that we propose in the Appendix, showing that the physical feedback Kq implemented by softness equips the soft robot with the ability of supporting torques τ_{r} without losing stability.

IV. Control of a Planar Soft Arm

In this section we consider the problem of controlling a soft planar arm, as the one in Fig. 1. We consider it to be 1m long. Its 1Kg weight is homogeneously distributed along the whole body. As discussed in Sec. II, its dynamics can be accurately described by discretization. We consider for simplicity the arm inextensible, and we approximate it as a sequence of small links connected through revolute joints [28]. 20 segments are taken into account here, with length 0.05m and weight 0.05Kg. The robot impedance is $K = 0.05 I \frac{\mathrm{N}}{\mathrm{rad}}$, $D = 0.005 I \frac{\mathrm{N\,s}}{\mathrm{rad}}$, where $I \in \mathbb{R}^{20\times 20}$ is the identity matrix. Note that all the results presented here are provided under the hypothesis of perfect knowledge of the system model and state.

We consider as task the end effector positioning. Thus $x \in \mathbb{R}^2$ is the end effector's position expressed in Cartesian coordinates (i.e. $m = 2$), and $h(q)$ is the robot's direct kinematics. The rest configuration (i.e. $q = 0$) is such that the robot is extended, with its end effector in position $x = [1, 0]^{\mathrm{T}}$m.

We propose to generate the control action in task space through the following direct extension of Khatib's Operational Space Controller [16]

$$\begin{aligned} f = {} & \Lambda_x(q)(\ddot{x}_{\mathrm{d}} + K_{\mathrm{d}}(\dot{x}_{\mathrm{d}} - \dot{x}) + K_{\mathrm{p}}(x_{\mathrm{d}} - x)) \\ & + \eta(q,\dot{q}) + J_B^{+\mathrm{T}}(q)\,(Kq + D\dot{q}) \end{aligned} \tag{22}$$

where K_{p} and K_{d} are the proportional and derivative gains. Remaining terms are defined as in (4).

Since $m = 2$, under hypothesis (21), only two synergies are sufficient to fully control x. We examine three ways of mapping the end effector force $f \in \mathbb{R}^2$ into joint space. The first two implement the here proposed strategy (20) with two different synergy matrices

$$\tau = S_{\mathrm{lp}}^{\mathrm{T}}\sigma\,, \quad \sigma = P_{S_{\mathrm{lp}},B}(q)J^{\mathrm{T}}(q)f \in \mathbb{R}^2 \tag{23}$$

$$\tau = S_{\mathrm{hp}}^{\mathrm{T}}\sigma\,, \quad \sigma = P_{S_{\mathrm{hp}},B}(q)J^{\mathrm{T}}(q)f \in \mathbb{R}^2\,, \tag{24}$$

where $S_{\mathrm{lp}} \in \mathbb{R}^{20\times 2}$ and $S_{\mathrm{hp}} \in \mathbb{R}^{20\times 2}$ are the two actuation patterns, defined in Fig. 3. As third map we consider (6). Once again, it is worth noticing that the dimensionality of $\{\tau \ \text{s.t.} \ \tau = J^{\mathrm{T}}(q)f, \ \forall f \in \mathbb{R}^2, \ q \in \mathbb{R}^n\}$ is in general n, i.e. the system is fully actuated (see Fig. 2(a)). Therefore this map serves as benchmark, to compare the performance of the two strongly under-actuated cases, with an upper bound defined by the practically unfeasible fully actuated one.

Performing standard manipulations, and considering that

$$\begin{aligned} & J_B^{+\mathrm{T}}(q)SP_{S,B}(q)J^{\mathrm{T}}(q) = \\ & \left(J\,B^{-1}\,J^{\mathrm{T}}\right)^{-1} JB^{-1}S\left(JB^{-1}S\right)^{-1} JB^{-1}J^{\mathrm{T}} = I\,, \end{aligned} \tag{25}$$

yields a same closed loop dynamics in task space for all the three projections

$$\ddot{e} + K_{\mathrm{d}}\dot{e} + K_{\mathrm{p}}e = 0\,, \tag{26}$$

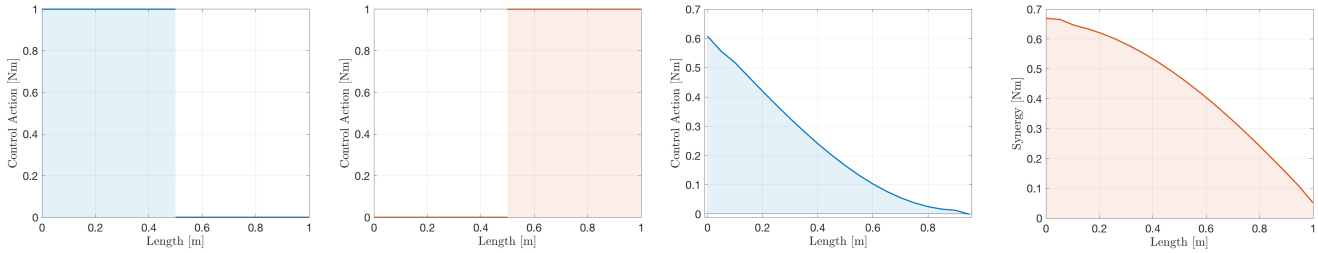

(a) S_{lp}, 1^{st} synergy (b) S_{lp}, 2^{nd} synergy (c) S_{hp}, 1^{st} synergy (d) S_{hp}, 2^{nd} synergy

Figure 3. Actuation patterns of a planar soft robot. The robot is 1m long. Each plot shows the amount of torque applied in each portion of the robot when an unitary synergistic input is applied. Two choices of synergistic matrix are considered here. Panels (a-b) depicts S_{lp}, wile panels (c-d) show S_{hp}.

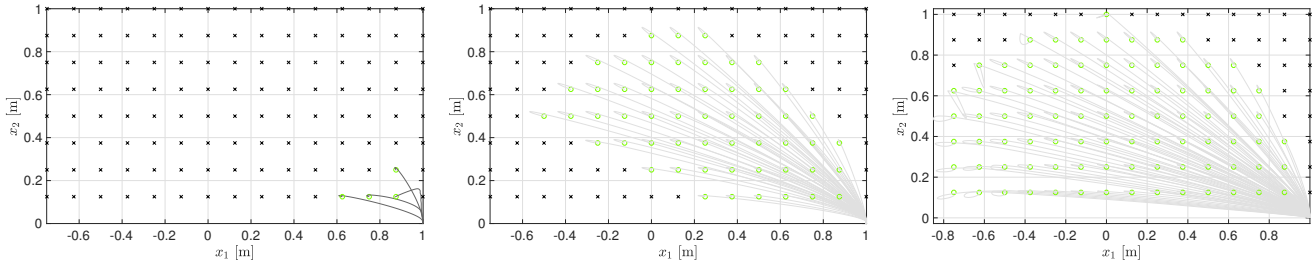

(a) S_{lp} (b) S_{hp} (c) Fully actuated, $S = I$

Figure 4. Areas reachable by the end effector of a planar soft limb. The robot is 1m long, and in rest is placed with its base in $x = (0, 0)$ and its tip in $x = (1, 0)$. The desired force at the end effector is specified by (22). The green circles are points that the robot is able to reach, while the black crosses are points that the robot is not. We show with thin grey lines the trajectories of the end effector in case of success. The behavior is analogous for negative values of x_2, so only positive values are portrayed. Panel (a) shows the results when S_{lp} is considered, and Panel (b) depicts the results when S_{hp} is implemented. In the latter case the reached portion of the operational space is comparable with the one obtained with a fully actuated system, as depicted in Panel (c).

where $e = x_{\mathrm{d}} - x$ is the tracking error. This linear dynamics is globally asymptotically stable in zero for all $K_{\mathrm{d}} \succ 0$, and $K_{\mathrm{p}} \succ 0$. This assures that the dynamic task is asymptotically fulfilled. Different choices of K_{d} and K_{p} produce a different transient behaviors. We implement here a decoupled over-damped transient, by choosing $K_{\mathrm{d}} = \sqrt{2} I \frac{\mathrm{N\,s}}{\mathrm{m}}$ and $K_{\mathrm{p}} = I \frac{\mathrm{N}}{\mathrm{m}}$, where $I \in \mathbb{R}^{2\times 2}$ is the identity matrix.

With the aim of extensively evaluating the performance of the proposed strategy, we consider a set of targets to be reached with the end effector, covering the whole workspace. Resulting performance are reported in Fig. 4. We show here only positive values of x_2 since the behavior is symmetrical for negative ones. Green circles indicate points that the robot is able to reach, while black crosses mark points out of reach. If a point has been reached, we report the full trajectory of the end effector.

Fig. 4(a) shows results for the synergistic space defined by S_{lp}. The robot is able to operate locally, successfully reaching close targets. Fig. 4(b) shows instead the closed loop behavior when S_{hp} is used. This choice of actuation pattern produces improved performances, with a much larger area of the operational space reached. This result is even more encouraging if compared to the fully actuated case in Fig. 4(c), which only slightly differs.

The proposed controller (22), together with (24), is also tested in the more dynamic scenario of catching a target moving according to the law

$$x_{\mathrm{d}}(t) = \begin{bmatrix} 0.75 + 0.25\,\sin(\omega t) \\ 0.2 + 0.2\,\cos(\omega t) \end{bmatrix}\ \mathrm{m}\,, \tag{27}$$

with $\omega = \frac{1}{\mathrm{s}}$. Fig. 5 shows some salient moments of the resulting behavior. Colors encode the magnitude of the torque τ applied along the robot, from dark blue encoding no activation to red encoding maximum activation. The red cross shows the current value of x_{d}. The control in synergistic space σ is depicted in Fig. 6(a), while the evolution in configuration space q is presented in Fig. 6(b). The corresponding evolution in task space is reported in Fig. 6(c), confirming that $x \simeq x_{\mathrm{d}}$ after about 7s. The root mean square tracking error in task space evaluated in a 60s time window is $0.068\mathrm{m}$.

V. Control of a Soft Arm in Space

To further test the effectiveness of proposed results we consider a 3D soft arm, modeled as a sequence of 20 segments. We neglect extension and torsion deformations. Thus each segment brings to the robot two degrees of deformation [28], described by the Denavit-Hartenberg parameters 1) $d = 0$, $a = 0$, $\alpha = \frac{\pi}{2}$, $\theta = q_{2i-1}$, 2) $d = 0$, $a = 0$, $\alpha = \frac{\pi}{2}$, $\theta = q_{2i-1}$. As in the previous section, the soft limb is 1m long, and it weights 1Kg. The weight is homogeneously distributed. The robot impedance is $K = 5I \frac{\mathrm{Nm}}{\mathrm{rad}}$, $D = 1I \frac{\mathrm{Nm\,s}}{\mathrm{rad}}$, where $I \in \mathbb{R}^{3\times 3}$ is the identity matrix. We consider as task space the three coordinates of the end effector. The controller derives directly from (22) by including gravity compensation $G(q)$. The system is under actuated as specified by the synergy matrix $S = J(\bar{q})$, with $\bar{q} = [\pi/40,\ -\pi/360\ \ldots\ \pi/40,\ -\pi/360]^{\mathrm{T}}\mathrm{rad}$. The control action $f \in \mathbb{R}^3$ is converted to the high dimensional torques

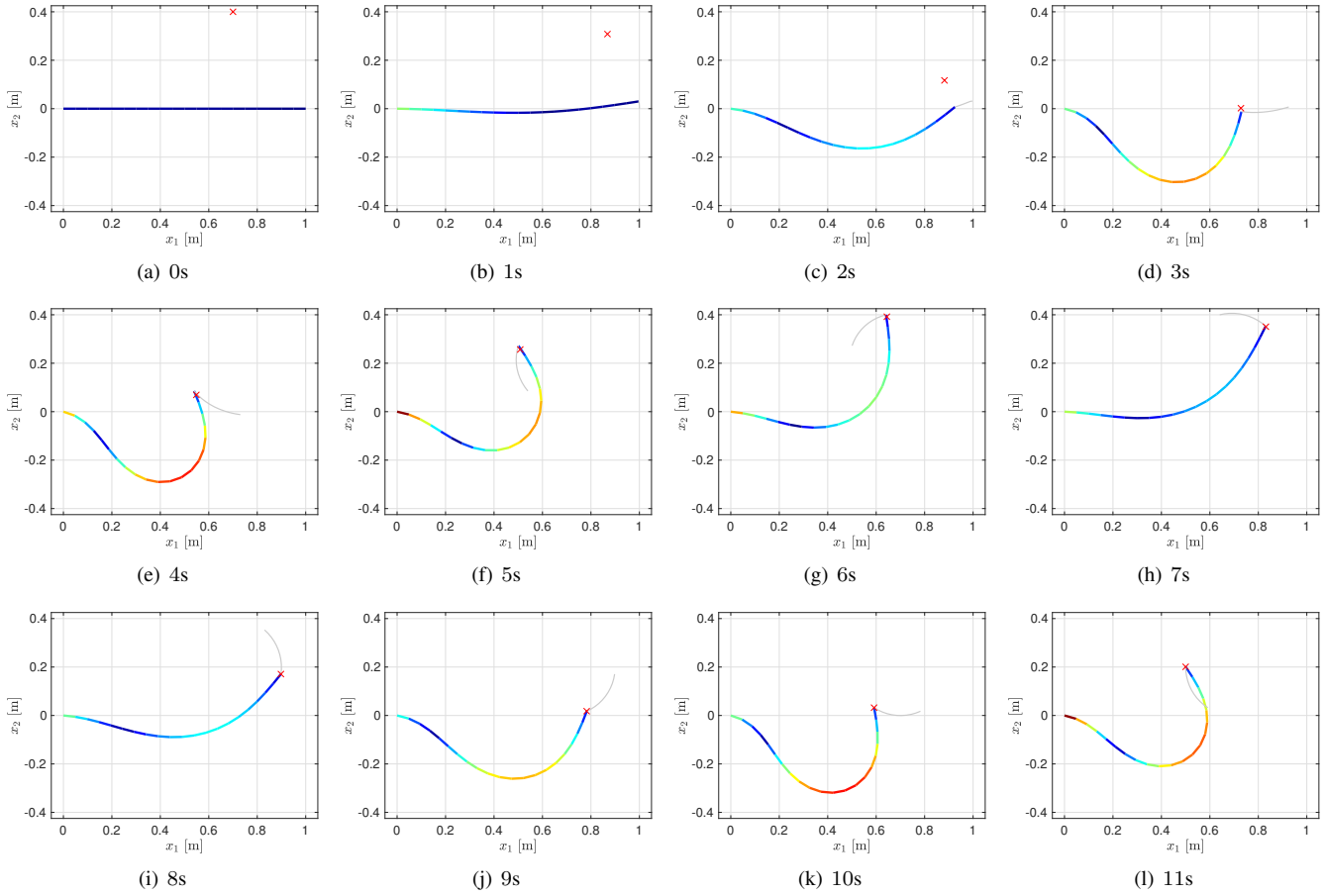

(a) 0s (b) 1s (c) 2s (d) 3s

(e) 4s (f) 5s (g) 6s (h) 7s

(i) 8s (j) 9s (k) 10s (l) 11s

Figure 5. Sequence of a soft limb catching a moving target in space. The target follows a circular trajectory, and it is graphically represented by a red cross. The robot is controlled through (22). The system is able to correctly perform the task with only two directions of actuation, defined by the synergies S_{hp}. The level of activation along the robot is encoded with colors. Red is the maximum torque, while blue is no torque.

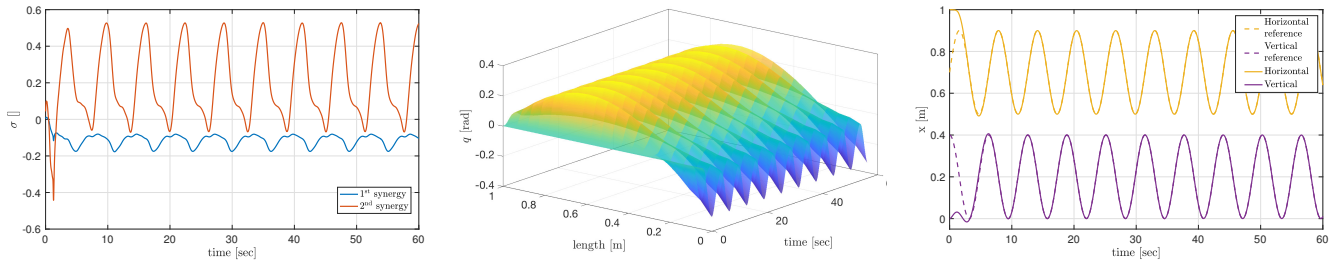

(a) Synergy weights (b) Robot's configuration (c) Task variables

Figure 6. Resulting behavior of the soft limb tracking with its tip the trajectory (27). Controller (22) and dynamically consistent projector in synergistic space $P_{S_{\mathrm{hp}},B}$ are used. Panel (a) shows the evolution of the two synergy weights σ commanded by the controller. They generate the evolution of configuration in time presented in Panel (b), and the evolution in task space in Panel (c). The robot behavior (solid lines) converges to the desired one (dotted lines) after about seven seconds.

through the dynamically consistent projector $P_{J(\bar{q}),B}$. In analogy with (22), we propose the controller

$$\tau = S\, P_{S,B}(q)[\Lambda_x(q)(\ddot{x}_{\mathrm{d}} + K_{\mathrm{d}}(\dot{x}_{\mathrm{d}} - \dot{x}) + K_{\mathrm{p}}(x_{\mathrm{d}} - x)) + \eta(q,\dot{q}) + J_B^{+\mathrm{T}}(q)\,(Kq + D\dot{q} + G(q))]\,. \tag{28}$$

Arguments analogous to the ones reported in the previous section yield a task space closed loop dynamics equivalent to (26). Thus, the convergence condition is again that both K_{d} and K_{p} are positive defined. We consider $K_{\mathrm{d}} = 10I\frac{\mathrm{N\,s}}{\mathrm{m}}$ and $K_{\mathrm{p}} = I\frac{\mathrm{N}}{\mathrm{m}}$, with $I \in \mathbb{R}^{3\times 3}$ being the identity matrix.

We present in Fig. 7 a sequence of the robot catching a dynamically moving target with coordinates

$$x_{\mathrm{d}}(t) = \begin{bmatrix} 0.7 \\ 0.3\,\cos(\omega t) \\ 0.3\,\sin(\omega t) \end{bmatrix} \mathrm{m}\,, \tag{29}$$

where $\omega = \frac{1}{\mathrm{s}}$. The system acquires the target with its end effector after about 7s and maintains it for the rest of the execution. The root mean square tracking error in task space evaluated in a 60s time window is $0.082\mathrm{m}$.

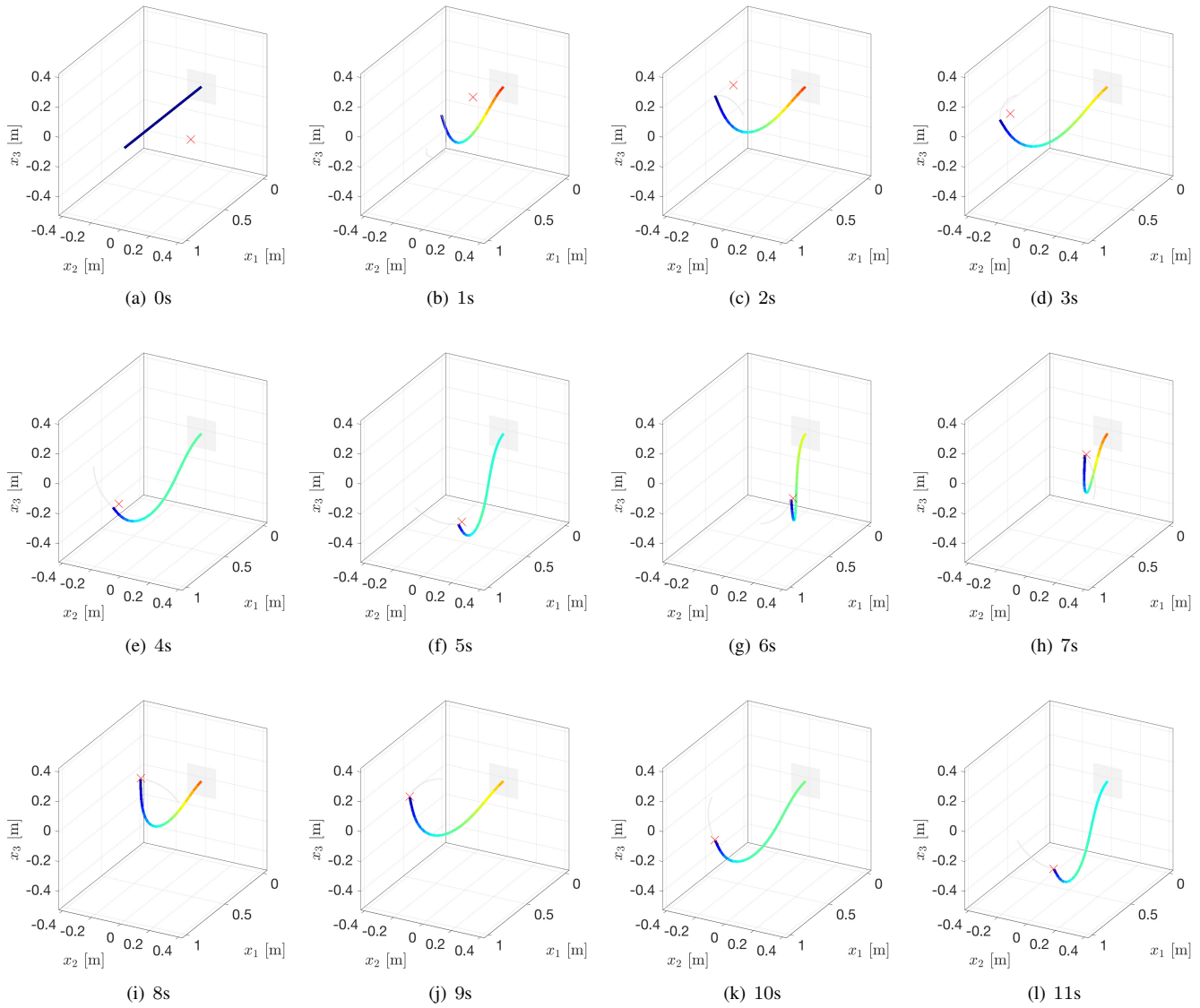

Figure 7. Sequence of a soft limb catching a moving target in space. The arm is free to move in 3D, and it is subject to a constant gravitational field. The target is graphically represented by a red cross. The robot is controlled through (22). The system is able to correctly perform the task with only three directions of actuation. The level of activation along the robot is encoded with colors. Red is the maximum torque, while blue is no torque.

VI. Conclusions and Future Work

This paper deals with the problem of controlling soft robots when only a reduced set of directions of actuation is available. In soft robots is indeed intrinsically impossible to work with a fully actuated input space without introducing strong approximations, while controllers developed for classic rigid-bodied robots often assume this property. We proved here that given a task of dimension m, a same number of synergies are sufficient to accomplish it under opportune hypotheses. We then introduced the *Dynamically Consistent Projector in Synergistic Space*. It enables adapting any controller designed into the task space, to generate control actions in the under-actuated input space. Finally we propose an extension of Khatib's operational space controller, using the proposed projector. The approach was extensively tested in simulation on two planar soft arms, and on a 3D soft arm experiencing gravity. Simulations show very good performance. However, the quality of the results changed substantially depending on the actuation pattern considered. We will investigate this aspect in future work, more specifically addressing the optimal design of S.

Given the nature of the present work, a perfect knowledge of the model has been hypothesized for the sake of space and readability. A formal evaluation of robustness is beyond the scope of this paper, and we postpone it to future work, together with the experimental validation of the algorithms. Note indeed that, to fill the gap between model-based control and experiments, also the problem dual to under-actuation must be tackled. Indeed, as it is unreasonable to pack a sufficient amount of actuators in a soft body to make it fully actuated, it is also very challenging to introduce sufficient sensors to make all the state directly measurable. This calls for the design of state observers able to estimate the full soft robot state from a reduced set of measurements.

APPENDIX: A NOTE ON SELF STABILIZATION

Consider a set of constants $M_{\mathrm{J},i}$,$M_{\mathrm{e},i}$,$M_{\mathrm{G}} \in \mathbb{R}^+$ such that

$$\left|\left|\frac{\mathrm{d}J_i}{\mathrm{d}q}\right|\right| < M_{\mathrm{J},i} \ , \quad \left|\left|\frac{\mathrm{d}J_{\mathrm{ext},i}}{\mathrm{d}q}\right|\right| < M_{\mathrm{e},i} \ , \quad \left|\left|\frac{\mathrm{d}G}{\mathrm{d}q}\right|\right| < M_{\mathrm{G}} \ , \tag{30}$$

where J_i and $J_{\mathrm{ext},i}$ are Jacobians associated to i-th output and contact point respectively, and G is the gravity field. Then the following proposition holds

Proposition 1. *The soft robot*

$$B(q)\ddot{q} + C(q,\dot{q})\dot{q} + G(q) + Kq + D\dot{q} = J^{\mathrm{T}}\bar{f} + \bar{\tau} + J^{\mathrm{T}}_{\mathrm{ext}}\bar{f}_{\mathrm{ext}} \tag{31}$$

is stable for all choices of $\bar{f} \in \mathbb{R}^m$, $\bar{\tau} \in \mathbb{R}^n$, and $\bar{f}_{\mathrm{ext}} \in \mathbb{R}^k$ such that

$$K \succ (\sum_i M_{\mathrm{J},i}\bar{f}_i + \sum_i M_{\mathrm{e},i}\bar{f}_{\mathrm{ext},i} + M_{\mathrm{G}})I \tag{32}$$

Proof. Let's call $q_{\mathrm{eq}} \in \mathbb{R}^n$ the equilibrium configuration, such that

$$Kq_{\mathrm{eq}} + G(q_{\mathrm{eq}}) = J^{\mathrm{T}}(q_{\mathrm{eq}})\bar{f} + \bar{\tau} + J^{\mathrm{T}}_{\mathrm{ext}}(q_{\mathrm{eq}})\bar{f}_{\mathrm{ext}} \ . \tag{33}$$

Subtracting (33) from (31) yields

$$\begin{aligned} B(q)\ddot{q} + C(q,\dot{q})\dot{q} + (G(q) - G(q_{\mathrm{eq}})) + K(q - q_{\mathrm{eq}}) + D\dot{q} = \\ (J^{\mathrm{T}}(q) - J^{\mathrm{T}}(q_{\mathrm{eq}}))\bar{f} + (J^{\mathrm{T}}_{\mathrm{ext}}(q) - J^{\mathrm{T}}_{\mathrm{ext}}(q_{\mathrm{eq}}))\bar{f}_{\mathrm{ext}} \ . \end{aligned} \tag{34}$$

We define

$$H(q) \triangleq G(q) - J^{\mathrm{T}}(q)\bar{f} - J^{\mathrm{T}}(q)\bar{f}_{\mathrm{ext}} \ , \tag{35}$$

obtaining the following dynamics

$$B(q)\ddot{q} + C(q,\dot{q})\dot{q} + H(q) = K(q_{\mathrm{eq}} - q) - D\dot{q} + H(q_{\mathrm{eq}}) \ . \tag{36}$$

This is equivalent to the dynamics of a rigid robot subject to a *gravity* field $H(q)$, and controlled through a PD plus constant gravity compensation. Thus we can prove the thesis from the same arguments of Th. 1 in [29]. Note indeed that $H(q)$ is limited by hypothesis, and that it admits the potential function

$$U(q) = U_{\mathrm{G}}(q) - h^{\mathrm{T}}(q)\bar{f} - h^{\mathrm{T}}_{\mathrm{ext}}(q)\bar{f}_{\mathrm{ext}} \ , \tag{37}$$

where $U_{\mathrm{G}} : \mathbb{R}^n \to \mathbb{R}$ is the gravity potential field, $h(q) : \mathbb{R}^n \to \mathbb{R}^m$ and $h_{\mathrm{ext}} : \mathbb{R}^n \to \mathbb{R}^k$ are the direct kinematics of the operational space and of the points of application of external forces respectively.

□

REFERENCES

[1] S. Kim, C. Laschi, and B. Trimmer, "Soft robotics: a bioinspired evolution in robotics," *Trends in biotechnology*, vol. 31, no. 5, pp. 287–294, 2013.

[2] D. Rus and M. T. Tolley, "Design, fabrication and control of soft robots," *Nature*, vol. 521, no. 7553, pp. 467–475, 2015.

[3] T. George Thuruthel, Y. Ansari, E. Falotico, and C. Laschi, "Control strategies for soft robotic manipulators: A survey," *Soft robotics*, 2018.

[4] R. J. Webster III and B. A. Jones, "Design and kinematic modeling of constant curvature continuum robots: A review," *The International Journal of Robotics Research*, vol. 29, no. 13, pp. 1661–1683, 2010.

[5] F. Renda, F. Boyer, J. Dias, and L. Seneviratne, "Discrete cosserat approach for multi-section soft robots dynamics," *arXiv preprint arXiv:1702.03660*, 2017.

[6] S. H. Sadati, S. E. Naghibi, I. D. Walker, K. Althoefer, and T. Nanayakkara, "Control space reduction and real-time accurate modeling of continuum manipulators using ritz and ritz–galerkin methods," *IEEE Robotics and Automation Letters*, vol. 3, no. 1, pp. 328–335, 2018.

[7] J. Chenevier, D. González, J. V. Aguado, F. Chinesta, and E. Cueto, "Reduced-order modeling of soft robots," *PloS one*, vol. 13, no. 2, p. e0192052, 2018.

[8] S. Grazioso, G. Di Gironimo, and B. Siciliano, "A geometrically exact model for soft continuum robots: The finite element deformation space formulation," *Soft robotics*, 2018.

[9] L. Sciavicco and B. Siciliano, *Modelling and control of robot manipulators*. Springer Science & Business Media, 2012.

[10] C. Della Santina, R. K. Katzschmann, A. Bicchi, and D. Rus, "Dynamic control of soft robots interacting with the environment," in *Proceedings of the 1st International Conference on Soft Robotics*, 2018.

[11] H. Hauser, A. J. Ijspeert, R. M. Füchslin, R. Pfeifer, and W. Maass, "Towards a theoretical foundation for morphological computation with compliant bodies," *Biological cybernetics*, vol. 105, no. 5-6, pp. 355–370, 2011.

[12] C. Della Santina, M. Bianchi, G. Grioli, F. Angelini, M. Catalano, M. Garabini, and A. Bicchi, "Controlling soft robots: balancing feedback and feedforward elements," *IEEE Robotics & Automation Magazine*, vol. 24, no. 3, pp. 75–83, 2017.

[13] C. Alessandro, I. Delis, F. Nori, S. Panzeri, and B. Berret, "Muscle synergies in neuroscience and robotics: from input-space to task-space perspectives," *Frontiers in computational neuroscience*, vol. 7, p. 43, 2013.

[14] G. Sumbre, G. Fiorito, T. Flash, and B. Hochner, "Neurobiology: motor control of flexible octopus arms," *Nature*, vol. 433, no. 7026, p. 595, 2005.

[15] C. Spinage, "Elephants," *T & AD Poyser, London*, p. 319, 1994.

[16] O. Khatib, "A unified approach for motion and force control of robot manipulators: The operational space formulation," *IEEE Journal on Robotics and Automation*, vol. 3, no. 1, pp. 43–53, 1987.

[17] M. B. Rubin, *Cosserat theories: shells, rods and points*. Springer Science & Business Media, 2013, vol. 79.

[18] S. Chiaverini, G. Oriolo, and A. Maciejewski, "Redundant manipulators," in *Springer handbook of robotics*. Springer, 2016, pp. 221–242.

[19] N. Mansard, O. Khatib, and A. Kheddar, "A unified approach to integrate unilateral constraints in the stack of tasks," *IEEE Transactions on Robotics*, vol. 25, no. 3, pp. 670–685, 2009.

[20] C. Ott, *Cartesian impedance control of redundant and flexible-joint robots*. Springer, 2008.

[21] K. J. Kim and S. Tadokoro, "Electroactive polymers for robotic applications," *Artificial Muscles and Sensors*, vol. 23, p. 291, 2007.

[22] C. Laschi, M. Cianchetti, B. Mazzolai, L. Margheri, M. Follador, and P. Dario, "Soft robot arm inspired by the octopus," *Advanced Robotics*, vol. 26, no. 7, pp. 709–727, 2012.

[23] A. D. Marchese, R. K. Katzschmann, and D. Rus, "A recipe for soft fluidic elastomer robots," *Soft Robotics*, vol. 2, no. 1, pp. 7–25, 2015.

[24] M. Mistry and L. Righetti, "Operational space control of constrained and underactuated systems," *Robotics: Science and systems VII*, pp. 225–232, 2012.

[25] K. B. Petersen, M. S. Pedersen *et al.*, "The matrix cookbook," *Technical University of Denmark*, vol. 7, no. 15, p. 510, 2008.

[26] F. Bosi, D. Misseroni, F. Dal Corso, S. Neukirch, and D. Bigoni, "Asymptotic self-restabilization of a continuous elastic structure," *Physical Review E*, vol. 94, no. 6, p. 063005, 2016.

[27] T. G. Thuruthel, E. Falotico, M. Manti, and C. Laschi, "Stable open loop control of soft robotic manipulators," *IEEE Robotics and Automation Letters*, 2018.

[28] R. S. Penning and M. R. Zinn, "A combined modal-joint space control approach for continuum manipulators," *Advanced Robotics*, vol. 28, no. 16, pp. 1091–1108, 2014.

[29] P. Tomei, "Adaptive pd controller for robot manipulators," *IEEE Transactions on Robotics and Automation*, vol. 7, no. 4, pp. 565–570, 1991.